Geoderma 407 (2022) 115564

Contents lists available at ScienceDirect

Geoderma

journal homepage: www.elsevier.com/locate/geoderma

Determining water content and bulk density: The heat-pulse method outperforms the thermo-TDR method in high-salinity soils

Wei Peng [a], Yili Lu [a,*], Mengmeng Wang [a], Tusheng Ren [a], Robert Horton [b]

[a] College of Land Science and Technology, China Agricultural University, Beijing 100193, China
[b] Department of Agronomy, Iowa State University, Ames, IA 50011, United States

ARTICLE INFO

Handling Editor: Morgan Cristine L.S.

Keywords:
Thermo-time domain reflectometry method
Heat-pulse method
Water content
Bulk density
Soil thermal properties

ABSTRACT

Heat-pulse (HP) and thermo-time domain reflectometry (thermo-TDR) methods have been used to determine soil thermal properties, water content (θ) and bulk density (ρ_b) simultaneously. Their performances on salt-affected soils, however, remain unknown. This study investigated the effect of salinity on HP signals and thermo-TDR measured electromagnetic waveforms, and the derived θ and thermal property values of packed soil columns with various textures, saturations and bulk electrical conductivities (σ_a). The thermo-TDR and HP-based methods for estimating ρ_b values were also evaluated. The results showed that: (1) at σ_a values lower than 1.0 dS m^{-1}, the TDR method provided reliable θ with relative errors within 5%; salt effects became apparent at σ_a values greater than 1.0 dS m^{-1} due to the distortion of TDR waveforms; the TDR method failed to estimate θ at $\sigma_a > 2.71$ dS m^{-1} because the 2nd reflection point on the waveform was undetectable; (2) salinity had negligible effects on soil thermal property values in the studied range ($\sigma_a < 7.59$ dS m^{-1}), and the HP-based approach was able to derive θ and ρ_b values from thermal property measurements, with root mean square errors within 0.02 m^3 m^{-3} for θ and within 0.12 Mg m^{-3} for ρ_b. Thus, the HP-based approach outperformed the thermo-TDR approach for determining θ and ρ_b values in soils with $\sigma_a > 1.0$ dS m^{-1}.

1. Introduction

Quantitative determination of soil water content (θ), thermal property values, electrical conductivity (σ_a) and bulk density (ρ_b) are required to characterize the physical state and transfer processes in salt-affected soils (Nassar et al., 1997; Nassar and Horton, 1999; Hamamoto et al., 2010). In saline soils, coupled transport processes of water and heat are accompanied by salt dissolution and precipitation which often lead to porosity variations (Olivella et al., 1996). Therefore, it is important to determine soil thermal property values, θ, σ_a, and ρ_b simultaneously to study coupled processes in salt-affected soils.

The heat-pulse (HP) method is widely used to determine soil thermal properties, i.e., soil heat capacity (C) and thermal conductivity (λ). A thermo-TDR sensor, which integrates HP and time domain reflectometry (TDR) functions, can measure in situ values of C, λ, θ, and σ_a (Ren et al., 1999). Thermo-TDR and HP techniques can also determine in situ ρ_b based on C and λ models that express soil thermal property dependence on θ and ρ_b (Ren et al., 2003a; Ren et al., 2003b; Liu et al., 2008; Lu et al., 2016; Lu et al., 2018). Therefore, with sensor determined C, λ and θ values, ρ_b can be derived from either a C model or a λ model (de Vries, 1963; Lu et al., 2014; Tian et al., 2016). Thermo-TDR and HP methods have been reported to provide in situ, non-destructive measurements of ρ_b in laboratory and field soils (Liu et al., 2008; Tian et al., 2018; Fu et al., 2019).

In saline soils, salts have influence on both dielectric and thermal properties of soil. The TDR technique measures the travel time of electromagnetic waves and determines the apparent dielectric constant (K_a) of a soil based on the travel time. Then θ_{TDR} can be derived from an empirical θ-K_a equation such as the Topp et al. (1980) equation. A soil complex dielectric constant is composed of a real component (i.e., K_a) and an imaginary component, which represents the ionic conductivity losses and relates to σ_a (Nigara et al., 2015; Kargas and Soulis, 2019). Therefore, the TDR waveforms from saline soils can be used to estimate σ_a (Muñoz-Carpena et al., 2005). The presence of salt mainly affects the imaginary component of a soil complex dielectric constant (Nigara et al., 2015). The effect of salt on K_a values is not clear.

For the TDR technique, θ_{TDR} and σ_a measurements are both based on the propagation/reflection of voltage signals along parallel waveguides (Noborio, 2001; Robinson et al., 2003; Jones et al., 2002; Wang et al., 2021). However, in soils with high electrical conductivity, it is

* Correspondence author.
E-mail address: luyili@cau.edu.cn (Y. Lu).

https://doi.org/10.1016/j.geoderma.2021.115564
Received 24 June 2021; Received in revised form 27 September 2021; Accepted 29 October 2021
Available online 8 November 2021

challenging to measure θ_{TDR} and σ_a due to the fact that salts alter the propagation speed and attenuate the energy of voltage signals significantly (Dalton, 1992; Sun et al., 2000; Nichol et al., 2002; Jones and Or, 2004; Schwartz et al., 2014). It is unlikely to determine θ_{TDR} accurately with high σ_a values in saline soils because salt affects the measurement of K_a (Regalado et al., 2007). It was reported that θ_{TDR} and K_a values were overestimated in soils with σ_a larger than 2 dS m^{-1} (Wyseure et al., 1997). Therefore, the errors in θ_{TDR} might cause errors in ρ_b and θ determination when applying the thermo-TDR method in salt-affected soils.

The presence of salt might affect soil thermal property values. There are contradictory reports about salt effects on soil λ. Researchers reported no apparent effects of solution concentrations of $CaCl_2$ up to 0.18 mol kg^{-1}, or with NaCl up to 0.34 mol kg^{-1} on λ of quartz sands (e.g., Van Rooyen and Winterkorn, 1959). However, Noborio and McInnes (1993) observed a reduction in soil λ with increasing soil solution concentrations ($CaCl_2$, $MgCl_2$, NaCl, or Na_2SO_4) from 0.10 mol kg^{-1} to solubility limits, because the increasing soil solution concentrations decreased the λ of soil solution, and chemical interactions between the soil solution and mineral particles, which could lead to the decrease of soil λ. Abu-Hamdeh and Reeder (2000) also found that soil λ decreased with increased concentrations of $CaCl_2$ and NaCl. Mochizuki et al. (2008) reported soil dependent-effects of salts on λ. For sand and non-swelling clay, λ remained stable or decreased with increasing NaCl concentration, while the λ of a swelling clay was unaffected by increasing NaCl concentrations. A complex mechanism involving many factors such as water content, salt content, and the differences in free water and salt solution affected the soil λ (Mochizuki et al., 2008). Also, little is known on the effect of salts on soil C values. So, it remains uncertain on how salts affect the determination of soil thermal properties and θ_{TDR}, as well as the consequences on ρ_b and porosity values derived from HP or thermo-TDR measurements. There is a need to determine the accuracy of HP and thermo-TDR methods to estimate soil property values in salt-affected soils.

In this study, a thermo-TDR sensor is used to determine θ, soil thermal property values and ρ_b in salt-affected soils. Our specific objectives are (1) to analyze the trends of electromagnetic waveforms as affected by soil salinity and its consequences on θ_{TDR} determination; (2) to examine the effect of salts on C and λ, and to determine the accuracy of ρ_b and θ values derived from thermo-TDR measurements as well as from HP measurements in salt-affected soils.

2. Theories

2.1. Determination of soil thermal property values, θ_{TDR} and σ_a with a thermo-TDR technique

A thermo-TDR sensor measures the HP signals (temperature rise with time data) and electromagnetic waveforms. To estimate soil thermal property values accurately, we used the theory of cylindrical-perfect-conductors to analyze the HP signals, which accounted for the finite probe radius and finite probe heat capacity (Knight et al., 2012; Peng et al., 2021). To determine θ_{TDR} and σ_a, the tangent line/second-order bounded mean oscillation model was used to analyze the electromagnetic waveforms and determine the reflection points and K_a values accurately (Wang et al., 2014, 2016). Then θ_{TDR} was determined from K_a with the Topp et al. (1980) equation.

For the derivation of σ_a, Heimovaara et al. (1995) provided the following equation,

$$\sigma_a = \frac{K_p}{R_{total} - R_c} f_T \tag{1}$$

where K_p is the cell constant of the probe (8.77 m^{-1}) which is calibrated with different KCl solutions (Heimovaara et al., 1995). R_{total} is the total resistance of the cable tester, coaxial cable, and probes, and it can be calculated from the amplitude of the TDR waveforms at very long times. Refer to the first section of the Supplemental Material for the calculation of R_{total} using Eq. (S1). R_c is the combined series resistance of the cable, connectors, and cable tester. Earlier studies reported that R_c was only a small fraction of the R_{total} (Huisman et al., 2008). Thus, in this study, we neglected R_c, and only used K_p and variable R_{total} to calculate σ_a.

The σ_a needs to be corrected with a temperature factor f_T (Heimovaara et al., 1995),

$$f_T = \frac{1}{1 + \mu(T - 25)} \tag{2}$$

in which μ is the temperature coefficient of the soil sample at the reference temperature of 25°C (0.0191°C^{-1}, Heimovaara et al., 1995), and T (°C) is the soil sample temperature at the measurement time.

2.2. Estimation of ρ_b values with the thermo-TDR and HP based methods

Based on quantitative relationships between values of C, λ and θ_{TDR}, thermo-TDR and HP based methods can be used to determine θ and ρ_b of salt-affected soils.

2.2.1. Thermo-TDR method to estimate ρ_b values

The de Vries (1963) C model, describing the linear relationship between C and θ, provides a way to determine in situ ρ_b (hereafter called the C-based thermo-TDR method, Ochsner et al., 2001; Ren et al., 2003a; Ren et al., 2003b),

$$\rho_b = \frac{C - \theta c_w}{c_s} \tag{3}$$

in which c_s (0.742 kJ kg^{-1} K^{-1}, Wang et al., 2019) is the specific heat capacity of soil solids, and c_w (4.18 kJ kg^{-1} K^{-1}, Campbell et al., 1991) is taken as the specific heat capacity of free water. With the Eq. (3), the ρ_b values are estimated directly with the thermo-TDR measured C and θ values.

The λ-based thermo-TDR method to determine ρ_b was developed with the purpose of eliminating the possibility of probe-deflection errors in C measurements (Lu et al., 2016; Tian et al., 2018). The empirical λ model from Lu et al. (2016) was adopted,

$$\begin{cases} \lambda = \lambda_{dry} + exp(\beta - \theta^{-\alpha}) \\ \alpha = 0.67 f_{cl} + 0.24 \\ \beta = 1.97 f_{sa} + 1.87\rho_b - 1.36 f_{sa}\rho_b - 0.95 \\ \lambda_{dry} = -0.56(1 - \rho_b/2.65) + 0.51 \end{cases} \tag{4}$$

where λ_{dry} (W m^{-1} K^{-1}) is the thermal conductivity of dry soil; α and β are shape factors determined by soil particle sizes and ρ_b, and f_{sa} and f_{cl} are the mass fractions of sand and clay particles under the USDA soil texture classification system. There is no explicit solution for ρ_b from Eq. (4), so after assigning an initial ρ_b of 1.0 Mg m^{-3}, an iterative approach is used to solve for ρ_b values using the nonlinear equation solver (f_{solve}) in MATLAB (Mathworks, Inc.) (Lu et al., 2017).

In this study, following Peng et al. (2019), a combination of the C-based and λ-based thermo-TDR approaches was used, i.e., the C-based approach was used when θ was less than 0.10 m^3 m^{-3}, and the λ-based approach was used when θ was greater than 0.10 m^3 m^{-3}. Both the C-based and the λ-based thermo-TDR approaches required a θ_{TDR} value to estimate ρ_b.

2.2.2. The HP-based approach to estimate θ_{HP} and ρ_b values

We also applied a HP-based method to estimate ρ_b values based solely on measured C and λ values without requiring a θ_{TDR} value (Lu et al., 2018). The HP-based method followed a three-step procedure to obtain θ_{HP} and ρ_b values (Lu et al., 2018). Step 1 included the rough estimation of θ_{HP} from a measured C value,

$$\theta_{HP} = \frac{C - \rho_b c_s}{c_w} \quad (5)$$

in which ρ_b (Mg m^{-3}) is an initial value assumed to be 1.5 Mg m^{-3} for coarse-textured soil with f_{sa} greater than 0.40 and a value of 1.0 Mg m^{-3} for fine-textured soils with f_{sa} less than 0.40 (Lu et al., 2018). In the second step, the approximate θ_{HP} value in Step 1 and the measured λ value were used to estimate the ρ_b value iteratively with Eq. (4). In step 3, the finial θ_{HP} value was re-calculated with Eq. (5) by using the updated ρ_b value obtained in Step 2.

3. Materials and methods

To evaluate the performance of HP-based and thermo-TDR-based methods in salt-affected soils, a thermo-TDR sensor was used to measure HP signals and electromagnetic waveforms on soil samples moistened with various concentrations of KCl solutions.

3.1. Thermo-TDR sensor configuration

The Peng et al. (2019) thermo-TDR sensor was selected for this study because it's heating probe rigidity, sharpened probe tips and thin sensing probes minimized soil disturbance and changes in probe spacing during sensor insertion. The thermo-TDR sensor has three parallel stainless-steel probes: one heater probe and two sensing probes with pointed tips that are mounted in a casting epoxy resin head. The probes are 70 mm long, and the heater probe and sensing probe have outer diameters of 2.38 mm and 2.00 mm, respectively. The spacing between the heater probe and each sensing probe is about 10 mm. Each sensing probe contains three thermocouples, positioned at 20, 35, and 50 mm away from the epoxy resin base. The inner conductor and the shield of the coaxial cable are soldered to the ends of the heater probe and the sensing probes, respectively.

3.2. Thermo-TDR sensor calibration

Prior to making measurements of soil thermal properties, θ_{TDR} and σ_a, the probe spacing, apparent probe length, and K_p of the thermo-TDR sensor were calibrated. The probe spacing was calibrated in agar-immobilized water (5 g L^{-1}) at 20°C by taking heat capacity of agar-immobilized water as 4.18 MJ m^{-3} K^{-1}, which assumed that heat capacity of water was not affected by the addition of agar (Campbell et al., 1991). A nonlinear regression method was used to fit the HP signals to inversely estimate probe spacing. The apparent probe length of the thermo-TDR sensor was calibrated by analyzing a TDR waveform in distilled water with apparent dielectric constant of water as 80.1 at 20°C (Haynes and Lide, 2010).

The K_p value was determined following the procedures of Heimovaara et al. (1995). TDR waveforms were collected after immersing the sensor in KCl solutions with the following concentrations: 0.0001, 0.0005, 0.001, 0.005, 0.01, 0.02, 0.1, and 1.0 mol L^{-1} (Fig. S2 in Supplemental material). Because R_{total} values could vary with KCl solution concentrations, TDR waveforms were used to calculate the variable R_{total} values. The electrical conductivity values for KCl solutions were measured with a conductivity meter (model DDS-307A, Shanghai INESA Scientific Instrument Co., China). Then K_p value of the thermo-TDR sensor was calculated by using regression analysis of electrical conductivity values vs. R_{total} (Ren et al., 1999).

3.3. Thermo-TDR measurements in salt-affected soils

Thermo-TDR measurements were made on three soils with varying textures (Table 1). Soil particle-size distributions of the studied soils were measured with the pipette method (Gee and Or, 2002). Soil samples were air-dried, crushed, and sieved through a 2-mm screen. Two different experimental methodologies: individual and continuous measurements were performed to explore the effects of salt on thermo-TDR measurements. For Soils 1 (sand) and 2 (loam) with individual measurements, disturbed samples were mixed thoroughly with either distilled water or KCl solutions of various concentrations and repacked uniformly into PVC columns (with a height of 80 mm and a diameter of 70 mm). The dry and wet packing procedures in Oliviera et al. (1996) were used as a reference to pack soil columns uniformly. Prior to packing a soil column, a soil sample was divided into four equal parts. One of the parts was poured into a cylinder to form a 2-cm thick layer. A 6-cm diameter cylindrical wooden rod was used to press the soil layer to a desired density, and the surface of the soil layer was lightly scratched to prevent stratification within the soil column. The packing steps were repeated with the other soil parts until the cylinder was filled. This produced a series of soil columns with σ_a ranging from 0.07 to 7.59 dS m^{-1} and θ values of 0.08, 0.15, 0.20 and 0.25 m^3 m^{-3}. The relatively small ρ_b ranges of the soil columns were 1.55 ± 0.05 Mg m^{-3} for Soil 1 and 1.35 ± 0.05 Mg m^{-3} for Soil 2, respectively, which was a result of careful packing. The soil columns were allowed to equilibrate at room temperature (20°C) before thermo-TDR measurements. Five repeated measurements were made on each column before the soil columns were oven dried at 105°C for 24 h to determine the actual θ and ρ_b values.

Table 1
Texture, particle size distribution and bulk density (ρ_b) of the repacked soils used in this study.

Texture	Particle size distribution			ρ_b
	2–0.05 mm	0.05–0.002 mm	<0.002 mm	
	%			Mg m^{-3}
Sand	94	1	5	1.50–1.60
Loam	48	38	14	1.24–1.40
Silt Loam	27	50	23	1.30

For Soil 3 (silt loam), continuous measurements in time were used to determine the dynamic θ and σ_a values. The sample was packed to a ρ_b of 1.30 Mg m^{-3} and was saturated from bottom to top with a 0.1 mol L^{-1} KCl solution. Two thermo-TDR sensors were inserted into the soil column horizontally at the depths of 20 mm and 60 mm. The saturated column was allowed to dry gradually with one end open to the atmosphere. During the evaporation process, a balance recorded the water loss hourly and a series of HP and TDR measurements were obtained over a 10-day period until the soil column mass approached a relatively constant value. The σ_a and θ values for the whole column were taken as the average of the readings from the two sensors.

To make a HP measurement, a current of 0.23 A was applied to the central heater probe with a direct current supply for 25 s to release heat energy, and temperature changes with time at the sensing probes were recorded for 480 s at a 1-s interval. The TDR measurements were made by using a TDR200 reflectometer (Campbell Scientific Inc., Logan, UT). The HP signals and TDR waveforms were recorded with a datalogger (model CR3000, Campbell Scientific Inc., Logan, UT). Based on the previously stated theories, soil thermal property, θ and σ_a data were derived from the HP signals and TDR waveforms, respectively. In this study, the average C and λ values were derived from measured HP datasets with the six thermocouples.

3.4. Error analysis

Soil thermal property values determined with the thermo-TDR measurements were compared to values obtained from the soil thermal property models, i.e. de Vries (1963) C model and Lu et al. (2014) λ model. The θ_{TDR}, θ_{HP} and ρ_b were compared to values obtained with the oven-dry method. Root mean square error (*RMSE*) and bias were used to evaluate the performances of the thermo-TDR and HP methods in salt-affected soils,

$$RMSE = \sqrt{\frac{\sum (x_e - x_m)^2}{n}} \quad (6)$$

$$\text{bias} = \frac{\sum (x_e - x_m)}{n} \quad (7)$$

where x_e represents the soil thermal property values, θ_{TDR}, θ_{HP} or ρ_b derived from thermo-TDR and HP methods, x_m represents thermal property values estimated with soil thermal property models or determined gravimetrically (i.e., oven-dried θ and ρ_b), n is the number of the values.

4. Results and discussion

In this section, we presented the analysis of the effects of salts on thermo-TDR sensor measured electromagnetic waveforms and on derived θ_{TDR} values. An approximate σ_a threshold value was determined for estimating θ_{TDR} with the TDR technique. Additionally, we evaluated the effects of salts on C and λ measurements, and the performances of thermo-TDR and HP-based methods to determine θ and ρ_b values in salt-affected soils.

4.1. Salt effects on thermo-TDR waveforms for determining θ_{TDR} values

Fig. 1 shows the recorded TDR waveforms from the thermo-TDR sensor on Soils 1, 2 and 3. For Soils 1 and 2, θ was in the range of 0.08–0.25 m^3 m^{-3}, and σ_a varied from 0.09 to 2.88 dS m^{-1} on the sand soil and from 0.07 to 6.02 dS m^{-1} on the loam soil (Fig. 1a-1b). For Soil 3, θ_{HP} values decreased from 0.37 to 0.20 m^3 m^{-3} and σ_a decreased from 2.71 to 1.08 dS m^{-1} during the 10-day monitoring period (Fig. 1c). It is apparent that the first reflection position L_1 remained constant (i.e., L_1 was unaffected by θ and σ_a), while the second reflection position L_2 varied significantly with θ and σ_a. Larger L_2 values were obtained at larger θ values, and L_2 became less identifiable as σ_a increased. This was attributed to the fact that for soil samples with high σ_a values, the electromagnetic signals were partially dissipated in the soils, which led to vagueness in the reflected TDR waveforms.

The final voltage amplitude of electromagnetic signals gradually decreased with increasing σ_a and were close to zero at σ_a of 22.5 dS m^{-1} (refer to Fig. S2 in the Supplemental material). The uncertainties in L_2 values at the higher salt concentrations usually led to relatively large errors in K_a and θ_{TDR} values (Dalton, 1992; Nichol et al., 2002). In this study, compared with the gravimetric θ values, the *RMSE* of θ_{TDR} values was 0.06 m^3 m^{-3} for the sand and loam soils, and 0.09 m^3 m^{-3} for the silt loam soil. A 0.01 m change in L_2 caused a θ_{TDR} error up to 0.02 m^3 m^{-3}. In addition, the relative error in θ_{TDR} estimates was σ_a dependent. It was within 5% when σ_a was less than 1.0 dS m^{-1}, and when σ_a values were larger than 1.0 dS m^{-1}, it reached 16% as σ_a increased. These results generally agreed with those from reports on other saturated and unsaturated saline soils (Wyseure et al., 1997; Sun et al., 2000; Topp et al., 2000). Besides, the effects of salt on the relationship of θ and K_a could not be neglected (Wyseure et al., 1997; Tan et al., 2018). Later, the θ-K_a equation in Topp et al. (1980) should be revisited for its accuracy to estimate θ in saline soils.

The attenuation of electromagnetic signals was influenced by several factors such as θ, soil texture, salinity, cable length and probe geometry (Jones et al., 2002). For TDR sensors, the waveform reflections (e.g., L_2) necessary for K_a measurements could be totally attenuated in soils with high σ_a values. It was reported that the negative effect of electrical conductivity on the amplitude of electromagnetic signals was reduced as the probe became shorter (Noborio et al., 2001; Nichol et al., 2002). Ren et al. (1999) gave a threshold value of 6.06 dS m^{-1} for a sensor with probe length of 40 mm. A much lower threshold value of 2 dS m^{-1} was reported for a sensor with a probe length of 160 mm (Nichol et al., 2002). For the thermo-TDR sensor used in this study, the L_2 values could not be clearly distinguished, and thus, they were unusable for θ_{TDR} estimations when σ_a was greater than 2.88 dS m^{-1} in the sand soil, 4.48 dS m^{-1} in the loam soil, and 2.71 dS m^{-1} in the silt loam soil (Fig. 1).

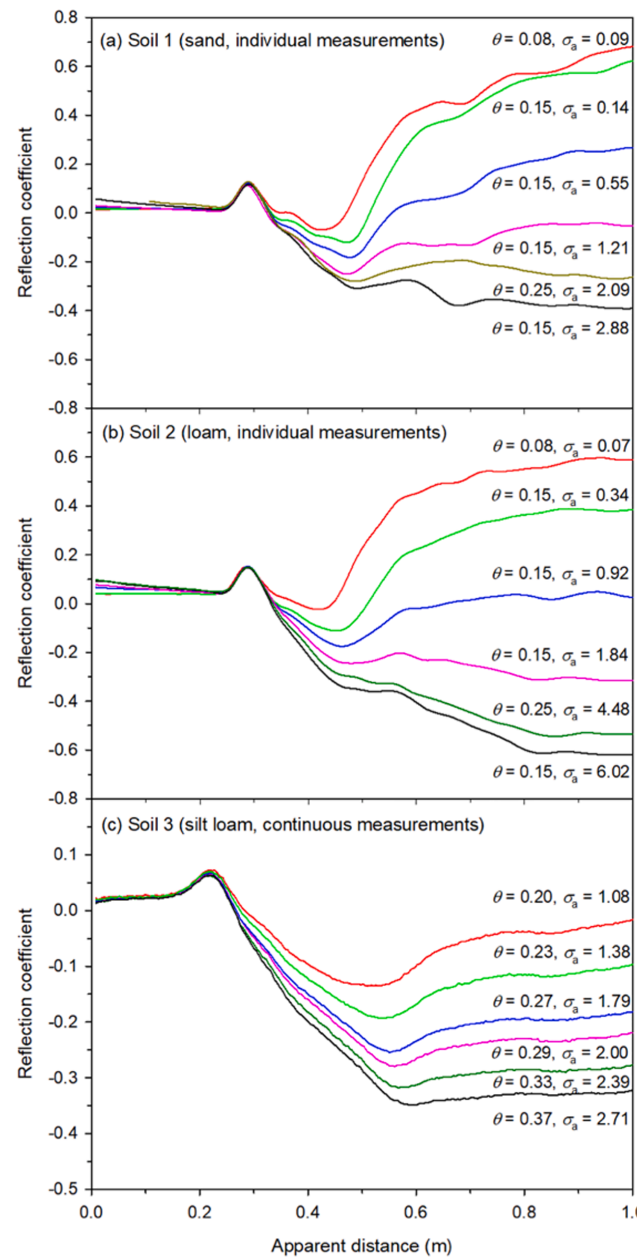

Fig. 1. Time domain reflectometry waveforms measured by thermo-TDR sensors for Soils 1–3 at specified water content values (θ, m^3 m^{-3}) and bulk soil electrical conductivity values (σ_a, dS m^{-1}).

4.2. Salt effects on thermo-TDR measured soil C and λ values

Fig. 2 presents measured and modeled C and λ values as a function of σ_a and θ for the sand and loam soils. The dashed curves represent the C values estimated with the de Vries (1963) model (Eq. (3)) and the λ values estimated with the Lu et al. (2014) model (Eq. (4)). The thermo-TDR measured C and λ results agreed well with the model estimates. For the conditions of this experiment, soil C and λ values varied significantly with θ, while not much changes in C and λ were observed with increasing σ_a. The strong variations in the measured C values might have resulted from probe spacing changes due to repeated insertion of the sensors into the soil samples (Fig. 2a-2b).

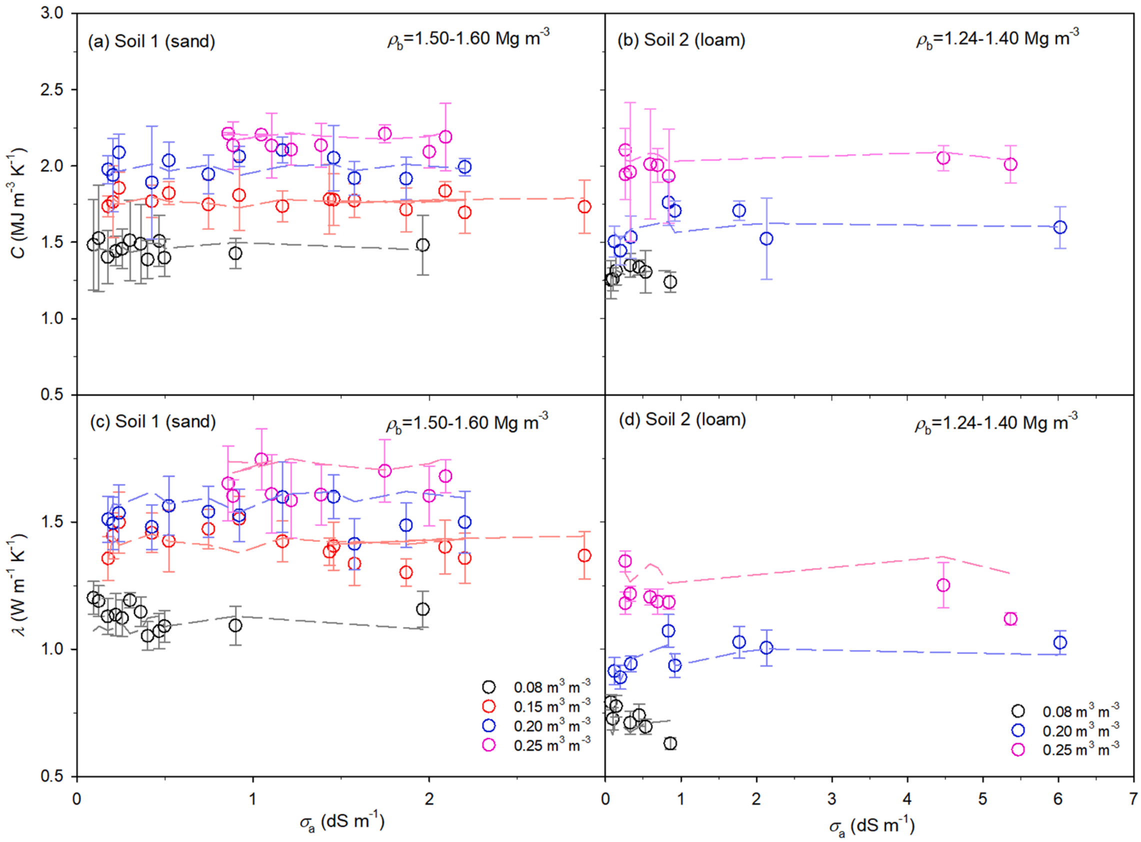

Fig. 2. Thermo-TDR sensor measured soil heat capacity (C) and thermal conductivity (λ) as a function of soil bulk electrical conductivity (σ_a) on the sand and loam soils at various water content and bulk density (ρ_b) values. The dashed curves are C or λ values estimated with the de Vries (1963) C model or the Lu et al. (2014) λ model. Each value represents the mean of five repeated measurements. The error bars indicate the standard deviations.

Controversial reports existed in the literature about salinity effects on soil thermal property values. In a quartz sand, Van Rooyen and Winterkorn (1959) reported no noticeable λ changes when $CaCl_2$ solution concentration was up to 0.18 mol kg^{-1} or NaCl solution concentration was up to 0.34 mol kg^{-1}, which agreed with our results that salts had negligible effects on C and λ measurements. However, Mochizuki et al. (2008) reported that increasing NaCl concentration (from 0 to 3 mol kg^{-1}) decreased the λ values of a sand and a non-swelling clay, but increased the λ values of glass beads in the middle to high θ range. Besides, we only performed experiments on soils with KCl solutions. Other salts such as NaCl, $CaCl_2$ and $MgCl_2$, differ in their interactions with clay particles, and might cause flocculation and aggregation in saline soils, which could lead to changes in soil λ (Abu-Hamdeh and Reeder, 2000). Thus, further research is needed to investigate the integrative effects of various salts, soil water, clay minerals, organic matter, as well as the structure (e.g., aggregation) on thermal properties of salt-affected soils.

4.3. *Determination of ρ_b and θ values of salt-affected soils with the HP and thermo-TDR based methods*

The determination of ρ_b and θ can be achieved with either HP-based or thermo-TDR based methods. Fig. 3 compares the derived ρ_b and θ estimates with the HP-based or thermo-TDR based methods to the directly measured mass determined values for soil cores with σ_a ranging from 0.07 to 7.59 dS m^{-1}. Compared to the directly measured mass determined ρ_b and θ values, the *RMSE*s were 0.18 Mg m^{-3} and 0.06 m^3 m^{-3} for the thermo-TDR estimated ρ_b and θ_{TDR} values, respectively (Fig. 3). As stated earlier, the θ_{TDR} errors were mainly caused by uncertain L_2 values, which limited the accuracy of θ_{TDR} and ρ_b estimates, resulting in several thermo-TDR estimated ρ_b and θ_{TDR} values to deviate from the 1:1 line. The application of the Topp et al. (1980) equation in saline soil might be another source of the θ_{TDR} errors. When σ_a values were less than 1 dS m^{-1}, the *RMSE*s of thermo-TDR estimated ρ_b and θ_{TDR} values were 0.12 Mg m^{-3} and 0.03 m^3 m^{-3}, respectively.

In contrast, the HP-based approach provided relatively accurate ρ_b and θ_{HP} values on these salt-affected soils (Fig. 3). The ρ_b and θ estimates generally agreed well with the directly measured mass determined values, as indicated by the even distribution of the data points around the 1:1 line. Error analysis showed that for the sand and loam soils, the ρ_b estimates had an average *RMSE* of 0.12 Mg m^{-3} and an average bias of -0.054 Mg m^{-3} (Fig. 3a), and the θ_{HP} estimates had a *RMSE* value of 0.02 m^3 m^{-3} and a bias of 0.008 m^3 m^{-3} (Fig. 3b). Some scattered outliers for HP determined θ values in Fig. 3b were observed, possibly due to the fact that HP determined θ values were prone to probe deflection errors, because they were directly derived from C values (Liu et al., 2020; Zhang et al., 2020). This type of error was insignificant for the in situ continuous measurements for Soil 3 (Fig. 4). Besides, it was found that there was a decrease in c_w with the addition of salt, and the specific heat capacity values of brine solutions decreased with increasing concentration and temperature (Sharqawy et al., 2010; Ramalingam and Arumugam, 2012). We determined that a 0.10 kJ kg^{-1} K^{-1} change in c_w caused a ρ_b error up to 0.34 Mg m^{-3} and a θ_{HP} error up to 0.01 m^3 m^{-3}. Thus, it is necessary to further investigate the appropriate c_w values used in Eqs. (3) and (5) for more accurate estimations of ρ_b and θ_{HP} values in salty soils.

The performance of the thermo-TDR based method to estimate θ and ρ_b values with σ_a less than 1 dS m^{-1} were similar to those for the HP-based method, however, the HP-based approach outperformed the thermo-TDR based approach for determining θ and ρ_b in salt-affected soils with σ_a ranging from 1.0 to 7.59 dS m^{-1}. The electromagnetic signal attenuated with increasing θ and σ_a, the large errors in thermo-TDR measured θ might be due to the undetectable L_2 values caused by

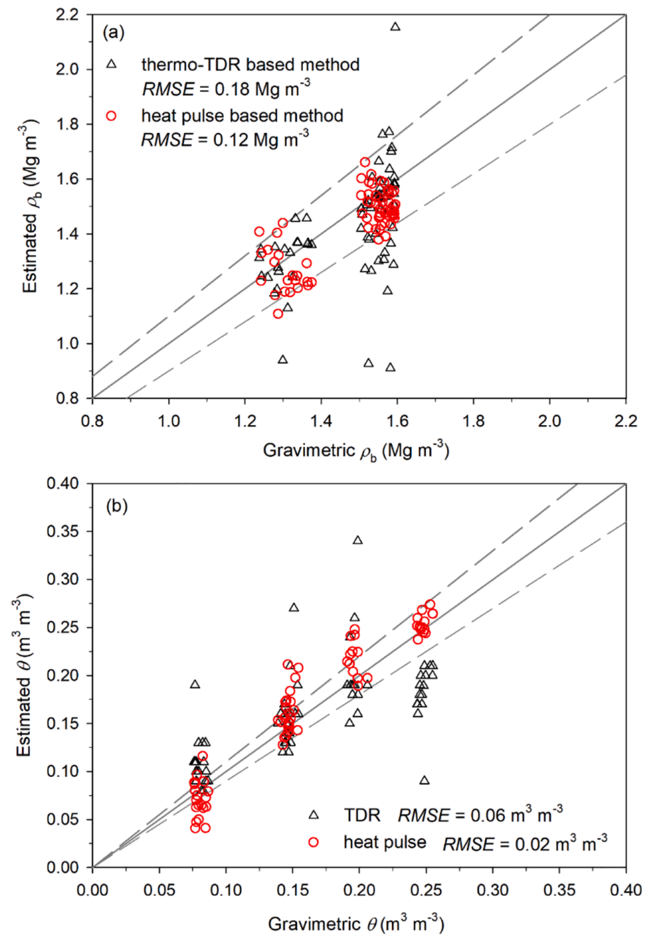

Fig. 3. Heat-pulse based (circles) and thermo-TDR based (triangles) estimates of (a) soil bulk density (ρ_b) and (b) water content (θ) versus directly measured ρ_b and θ values on the sand and loam soils. Soil bulk electrical conductivity ranged from 0.09 to 2.88 dS m^{-1} for the sand soil, and from 0.07 to 7.59 dS m^{-1} for the loam soil. The solid lines are the 1:1 lines, and the dashed lines are ±10% error lines.

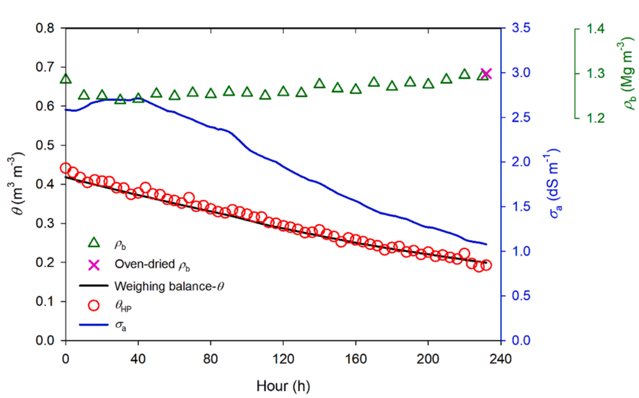

Fig. 4. Dynamics of soil water content (θ), bulk electrical conductivity (σ_a), and bulk density (ρ_b) values for Soil 3 during a drying process. The black line represents θ determined from mass balance measurements, while the red circles and green triangles are the heat-pulse based θ_{HP} and ρ_b estimates, respectively. The pink X represents the oven-dried ρ_b value. The blue line represents thermo-TDR measured σ_a. (For interpretation of the references to colour in this figure legend, the reader is referred to the web version of this article.)

the presence of salt, causing further large ρ_b errors. Thus, it was possible to obtain more accurate ρ_b and θ results from the HP-based approach than from the thermo-TDR approach, because salt effects on the C and λ measurements were negligible for the studied σ_a range (Fig. 2).

The HP-based θ_{HP} and ρ_b estimates were also examined on Soil 3 (Fig. 4). The average θ_{HP}, σ_a and soil thermal property values from the two thermo-TDR sensors were used to reduce the measurement errors caused by any nonuniform water and salt distributions in soil during the evaporation process. Due to uncertainty in waveform L_2 values (Fig. 1c), θ_{TDR} was overestimated with a *RMSE* of 0.09 m^3 m^{-3} (data not shown). Thus, only the HP-based results (θ_{HP} and ρ_b) were presented. During the evaporation process, θ decreased gradually from saturation to about 0.20 m^3 m^{-3}, and σ_a was reduced from 2.71 to 1.08 dS m^{-1} (Fig. 4). The θ_{HP} values followed closely to the θ trend from the mass balance measurements, with a *RMSE* of 0.01 m^3 m^{-3} and a bias of 0.001 m^3 m^{-3}. Meanwhile, σ_a decreased nonlinearly as θ decreased. The relatively constant ρ_b values indicated that there were no apparent soil structure changes during the drying process, and the estimated values matched well with the directly measured value (which was determined by oven drying soil at the end of the experiment). Hence, the HP measurements obtained with the thermo-TDR sensor provided reliable θ and ρ_b values on the salt-affected column of Soil 3. Generally, if you make measurements with a thermo-TDR sensor, both the thermo-TDR and HP-based methods can be used to estimate θ and ρ_b in salt-affected soils, but if σ_a is larger than 1.0 dS m^{-1}, we recommend using the HP-based method to estimate θ and ρ_b.

5. Conclusion

We evaluated the effects of salt concentration on thermo-TDR and HP-based methods to determine θ, ρ_b, σ_a and thermal property values in salt-affected soils. The presence of salts reduced the final voltage values after multiple reflections of electromagnetic waves, which decreased with increasing σ_a. When the σ_a value was greater than 1.0 dS m^{-1}, the distortion of TDR waveforms caused errors in L_2 estimations, which transferred to uncertainties in θ_{TDR}. It became difficult to determine θ_{TDR} values at relatively large σ_a values (>2.71 dS m^{-1}) because L_2 on the waveform was undetectable. Within the studied σ_a range (<7.59 dS m^{-1}), the effects of salt on soil thermal property values (C and λ) were negligible. The derived soil thermal property values could be used with the HP-based method to accurately estimate θ and ρ_b values, with *RMSE*s of 0.02 m^3 m^{-3} and 0.12 Mg m^{-3}, respectively. Generally, the thermo-TDR method could be used to determine reliable θ and ρ_b values when σ_a was less than 1.0 dS m^{-1}. For soils with σ_a ranging from 1.0 to 7.59 dS m^{-1}, the HP method outperformed the thermo-TDR method at determining accurate θ and ρ_b values. This has important implications for studies of coupled processes of water, heat and solute in soils. Future studies should focus on the performance of the HP method to determine θ and ρ_b values under complex field conditions.

Declaration of Competing Interest

The authors declare that they have no known competing financial interests or personal relationships that could have appeared to influence the work reported in this paper.

Acknowledgements

This research was supported by the National Natural Science Foundation of China (41977011 and 41671223), the U.S. National Science Foundation (2037504) and USDA-NIFA Multi-State Project 4188.

Appendix A. Supplementary data

Supplementary data to this article can be found online at https://doi.org/10.1016/j.geoderma.2021.115564.

References

Abu-Hamdeh, N.H., Reeder, R.C., 2000. Soil thermal conductivity: Effects of density, moisture, salt concentration, and organic matter. Soil Sci. Soc. Am. J. 64 (4), 1285–1290.

Campbell, G.S., Calissendorff, C., Williams, J.H., 1991. Probe for measuring soil specific heat using a heat-pulse method. Soil Sci. Soc. Am. J. 55 (1), 291–293.

Dalton, F.N., 1992. Development of time-domain reflectometry for measuring soil water content and bulk soil electrical conductivity, In: Topp, G.C., Reynodes, W.D., Green, R.E. (Eds.), Advances in measurement of soil physical properties: bringing theory into practice. SSSA Spec Publ. Soil Science Society of America, Madison, pp. 143–167.

de Vries, D.A., 1963. Thermal properties of soils. In: Van Wijk, W.R. (Ed.), Physics of plant environment. North-Holland Publishing Company, Amsterdam, pp. 210–235.

Fu, Y., Tian, Z., Amoozegar, A., Heitman, J., 2019. Measuring dynamic changes of soil porosity during compaction. Soil Till. Res. 193, 114–121.

Gee, G.W., Or, D., 2002. Particle-size analysis. In: Dane, J.H., Topp, G.C. (Eds.), Methods of Soil Analysis. Part 4–Physical Methods. Soil Science Society of America, Madison, pp. 255–294.

Hamamoto, S., Moldrup, P., Kawamoto, K., Komatsu, T., 2010. Excluded-volume expansion of Archie's law for gas and solute diffusivities and electrical and thermal conductivities in variably saturated porous media. Water Resour. Res. 46, W06514.

Haynes, W.M., Lide, D.R., 2010. CRC handbook of chemistry and physics: A ready-reference book of chemical and physical data, 97th ed. CRC Press, Boca Raton, FL.

Heimovaara, T.J., Focke, A.G., Bouten, W., Verstraten, J.M., 1995. Assessing temporal variations in soil water composition with time domain reflectometry. Soil Sci. Soc. Am. J. 59 (3), 689–698.

Huisman, J.A., Lin, C.P., Weihermüller, L., Vereecken, H., 2008. Accuracy of bulk electrical conductivity measurements with time domain reflectometry. Vadose Zone. J. 7 (2), 426–433.

Jones, S.B., Or, D., 2004. Frequency domain analysis for extending time domain reflectometry water content measurement in highly saline soils. Soil Sci. Soc. Am. J. 68 (5), 1568–1577.

Jones, S.B., Wraith, J.M., Or, D., 2002. Time domain reflectometry measurement principles and applications. Hydrol. Process. 16 (1), 141–153.

Kargas, G., Soulis, K.X., 2019. Performance evaluation of a recently developed soil water content, dielectric permittivity, and bulk electrical conductivity electromagnetic sensor. Agric. Water Mgt. 213, 568–579.

Knight, J.H., Kluitenberg, G.J., Kamai, T., Hopmans, J.W., 2012. Semianalytical solution for dual-probe heat-pulse applications that accounts for probe radius and heat capacity. Vadose Zone. J. 11 (2) https://doi.org/10.2136/vzj2011.0112.

Liu, G., Lu, Y.L., Wen, M.M., Ren, T.S., Horton, R., 2020. Advancing in the heat-pulse technique: Improvements in measuring soil thermal properties. Soil Sci. Soc. Am. J. 84, 1361–1370.

Liu, X., Ren, T., Horton, R., 2008. Determination of soil bulk density with thermo-time domain reflectometry sensors. Soil Sci. Soc. Am. J. 72 (4), 1000–1005.

Lu, Y., Horton, R., Ren, T., 2018. Simultaneous determination of soil bulk density and water content: a heat pulse-based method. Eur. J. Soil Sci. 69 (5), 947–952.

Lu, Y., Liu, X., Heitman, J., Horton, R., Ren, T., 2016. Determining soil bulk density with thermo-time domain reflectometry: a thermal conductivity based approach. Soil Sci. Soc. Am. J. 80 (1), 48–54.

Lu, Y.L., Liu, X.N., Zhang, M., Heitman, J.L., Horton, R., Ren, T.S., 2017. Thermo-time domain reflectometry method: advances in monitoring in situ soil bulk density. In: Logsdon, S. (Ed.), Methods of Soil Analysis, Volume 2. Soil Science Society of America, Madison, WI.

Lu, Y., Lu, S., Horton, R., Ren, T., 2014. An empirical model for estimating soil thermal conductivity from texture, water content, and bulk density. Soil Sci. Soc. Am. J. 78 (6), 1859–1868.

Mochizuki, H., Mizoguchi, M., Miyazaki, T., 2008. Effects of NaCl concentration on the thermal conductivity of sand and glass beads with moisture contents at levels below field capacity. J. Soil Sci. Plant Nutr. 54 (6), 829–838.

Muñoz-Carpena, R., Regalado, C.M., Ritter, A., Alvarez-Benedí, J., Socorro, A.R., 2005. TDR estimation of electrical conductivity and saline solute concentration in a volcanic soil. Geoderma. 124 (3-4), 399–413.

Nassar, I.N., Horton, R., 1999. Salinity and compaction effects on soil water evaporation and water and solute distributions. Soil Sci. Soc. Am. J. 63 (4), 752–758.

Nassar, I.N., Shafey, H.M., Horton, R., 1997. Heat, water, and solute transfer in unsaturated soil: II-Compacted soil beneath plastic cover. Transp. Porous Med. 27, 39–55.

Nichol, C., Beckie, R., Smith, L., 2002. Evaluation of uncoated and coated time domain reflectometry probes for high electrical conductivity systems. Soil Sci. Soc. Am. J. 66 (5), 1454–1465.

Nigara, T., Ding, J., Yu, D., 2015. Dielectric properties of saline soil based on a modified Dobson dielectric model. J. Arid Land. 7 (5), 696–705.

Noborio, K., 2001. Measurement of soil water content and electrical conductivity by time domain reflectometry: A review. Comput. Electron. Agric. 31 (3), 213–237.

Noborio, K., McInnes, K.J., 1993. Thermal conductivity of salt-affected soils. Soil Sci. Soc. Am. J. 57 (2), 329–334.

Ochsner, T.E., Horton, R., Ren, T., 2001. Simultaneous water content, air-filled porosity, and bulk density measurements with thermo-time domain reflectometry. Soil Sci. Soc. Am. J. 65 (6), 1618–1622.

Oliviera, I.B., Demond, A.H., Salehzadeh, A., 1996. Packing of sands for the production of homogeneous porous media. Soil Sci. Soc. Am. J. 60 (1), 49–53.

Olivella, S., Carrera, J., Gens, A., Alonso, E.E., 1996. Porosity variations in saline media caused by temperature gradients coupled to multiphase flow and dissolution/precipitation. Transp. Porous Med. 25 (1), 1–25.

Peng, W., Lu, Y.L., Ren, T.S., Horton, R., 2021. Application of infinite line source and cylindrical-perfect-conductor theories to heat pulse measurements with large sensors. Soil Sci. Soc. Am. J. https://doi.org/10.1002/saj2.20250.

Peng, W., Lu, Y., Xie, X., Ren, T., Horton, R., 2019. An improved thermo-TDR technique for monitoring soil thermal properties, water content, bulk density, and porosity. Vadose Zone. J. 18 (1), 1–9.

Ramalingam, A., Arumugam, S., 2012. Experimental study on specific heat of hot brine for salt gradient solar pond application. Int. J. Chemtech Res. 4, 956–961.

Regalado, C.M., Ritter, A., Rodríguez-González, R.M., 2007. Performance of the commercial WET capacitance sensor as compared with Time Domain Reflectometry in volcanic soils. Vadose Zone J. 6 (2), 244–254.

Ren, T., Noborio, K., Horton, R., 1999. Measuring soil water content, electrical conductivity, and thermal properties with a thermo-time domain reflectometry probe. Soil Sci. Soc. Am. J. 63 (3), 450–457.

Ren, T., Ochsner, T.E., Horton, R., 2003a. Development of thermo-time domain reflectometry for vadose zone measurements. Vadose Zone. J. 2 (4), 544–551.

Ren, T., Ochsner, T.E., Horton, R., Ju, Z., 2003b. Heat-Pulse method for soil water content measurement: Influence of the specific heat of the soil solids. Soil Sci. Soc. Am. J. 67 (6), 1631–1634.

Robinson, D.A., Jones, S.B., Wraith, J.M., Or, D., Friedman, S.P., 2003. A review of advances in dielectric and electrical conductivity measurement in soils using time domain reflectometry. Vadose Zone. J. 2 (4), 444–475.

Schwartz, R.C., Casanova, J.J., Bell, J.M., Evett, S.R., 2013. A reevaluation of time domain reflectometry propagation time determination in soils. Vadose Zone. J. 13.

Sharqawy, M.H., Lienhard, J.H., Zubair, S.M., 2010. Thermophysical properties of seawater: a review of existing correlations and data. Desalin. Water Treat. 16 (1-3), 354–380.

Sun, Z.J., Young, G.D., McFarlane, R.A., Chambers, B.M., 2000. The effect of soil electrical conductivity on moisture determination using time-domain reflectometry in sandy soil. Can. J. Soil Sci. 80 (1), 13–22.

Tan, X., Wu, J., Huang, J., Wu, M., Zeng, W., 2018. Design of a new TDR probe to measure water content and electrical conductivity in highly saline soils. J. Soil Sediments. 18 (3), 1087–1099.

Tian, Z., Lu, Y., Horton, R., Ren, T., 2016. A simplified de Vries-based model to estimate thermal conductivity of unfrozen and frozen soil. Eur. J. Soil Sci. 67 (5), 564–572.

Tian, Z., Lu, Y., Ren, T., Horton, R., Heitman, J.L., 2018. Improved thermo-time domain reflectometry method for continuous in-situ determination of soil bulk density. Soil Till. Res. 178, 118–129.

Topp, G.C., Davis, J.L., Annan, A.P., 1980. Electromagnetic determination of soil water content: measurements in coaxial transmission lines. Water Resour. Res. 16 (3), 574–582.

Topp, G.C., Zegelin, S., White, I., 2000. Impacts of the real and imaginary components of relative permittivity on time domain reflectometry measurements in soils. Soil Sci. Soc. Am. J. 64 (4), 1244–1252.

Van Rooyen, M., Winterkorn, H.F., 1959. Structural and textural influences on thermal conductivity of soils. In Proc. Annu. Meeting 38th. Highway Resources Board, Natl. Resources. Council, Washington, pp. 576–621.

Wang, Y., Lu, Y., Horton, R., Ren, T., 2019. Specific heat capacity of soil solids: Influences of clay content, organic matter and tightly bound water. Soil Sci. Soc. Am. J. 83 (4), 1062–1066.

Wang, Z., Kojima, Y., Lu, S., Chen, Y., Horton, R., Schwartz, R.C., 2014. Time domain reflectometry waveform analysis with second order bounded mean oscillation. Soil Sci. Soc. Am. J. 78 (4), 1146–1152.

Wang, Z., Lu, Y., Kojima, Y., Lu, S., Zhang, M., Chen, Y., Horton, R., 2016. Tangent line/second-order bounded mean oscillation waveform analysis for short TDR probe. Vadose Zone. J. 15 (1), 1–7.

Wang, Z., Timlin, D., Kojima, Y., Luo, C., Chen, Y., Li, S., Fleisher, D., Tully, K., Reddy, V. R., Horton, R., 2021. A piecewise analysis model for electrical conductivity calculation from time domain reflectometry waveforms. Comput. Electron. Agric. 182, 106012. https://doi.org/10.1016/j.compag.2021.106012.

Wyseure, G.C.L., Mojid, M.A., Malik, M.A., 1997. Measurement of volumetric water content by TDR in saline soils. Eur. J. Soil Sci. 48, 347–354.

Zhang, M., Lu, Y., Ren, T., Horton, R., 2020. In-situ probe spacing calibration improves the heat pulse method for measuring soil heat capacity and water content. Soil Sci. Soc. Am. J. 84 (5), 1620–1629.